Bulletin of the Seismological Society of America. Vol. 65, No. 6, pp. 1863–1885. December 1975

TWO-DIMENSIONAL, ANTIPLANE, BUILDING-SOIL-BUILDING INTERACTION FOR TWO OR MORE BUILDINGS AND FOR INCIDENT PLANE *SH* WAVES

BY H. L. WONG AND M. D. TRIFUNAC

ABSTRACT

Two-dimensional *SH*-type vibration of several shear walls erected on an elastic, homogeneous, half-space has been studied. The choice of the cylindrical coordinate system, suitable for analysis of rigid foundations with semi-circular cross section, has lead to the exact infinite series solution, which is ideal for the analysis of the physical nature of this problem and its dependence on several key parameters.

It has been shown that the presence of neighboring buildings may change the nature of the single soil-structure interaction problem appreciably and that scattering, diffraction, and interference of waves from and around several foundations with the incident *SH* waves can lead to significant shielding, as well as amplification of input motion for any of the buildings in a group. The effects of relative size of two, three and several foundations and their separation distances have been studied and presented in some detail.

INTRODUCTION

Many important buildings are located in metropolitan areas where they are surrounded by numerous other structures at small and large distances. The published analyses which consider soil-structure interaction, however, mostly consist of just one building or one foundation on top of a half-space (e.g., Luco and Westmann, 1971), while the problem of interaction of many buildings has, so far, not been studied. The interaction of two foundations has been explored analytically by Warburton *et al.* (1971) and experimentally by MacCalden (1969). Their models consisted of two rigid circular foundations placed on top of an elastic half-space. For antiplane vibrations, Luco and Contesse (1973) studied the interaction of two embedded foundations with semi-circular cross sections excited by vertically incident harmonic *SH* waves. Liang (1974) solved the related plain strain problem using the finite element approach. Interaction of three buildings in a three-dimensional setting has been studied by Lee and Wesley (1973).

The study of Luco and Contesse (1973) indicated that additional interaction effects caused by the presence of another structure may be important at low frequencies and near the fixed-based natural frequencies of the neighboring structure. However, some additional effects involving nonvertically incident *SH*-waves were not considered. In that case, the interaction will include the effect of shielding for the shear wall in the rear and amplification or deamplification for the shear wall in the front.

The purpose of this paper is, therefore, to investigate further the significance of the angle of incidence, the effect of the relative size and natural frequencies of neighboring structures, and the influence the separation distance may have on the interaction of two or more shear walls. These additional effects could become quite important at certain frequencies, and there may exist noticeable increases in the amplitude of foundation response caused by building-soil-building interaction.

The study of the interaction of two shear walls has been extended to cover the cases where many semi-circular foundations are present (Figure 1). The specially chosen geometry of the boundaries involved allows the boundary-value problem to be solved exactly by the method of separation of variables.

Numerical results of the exact solution indicate that the spacing between foundations can have a prominent effect on the response amplitudes. For smaller structures, new "natural frequencies" are being created by interference of the waves scattered from its larger neighbors. These "natural frequencies" are highly dependent upon the spacings of two or more foundations.

The Model and the Coordinate System

The scattered waves from the semi-cylindrical rigid foundations, $p = 1, 2, \ldots, N$, welded to the half-space ($y_1 \leqq 0$), are conveniently represented by polar coordinates (r_p, ϕ_p) which have their origins at the center of each foundation (Figure 1). Having

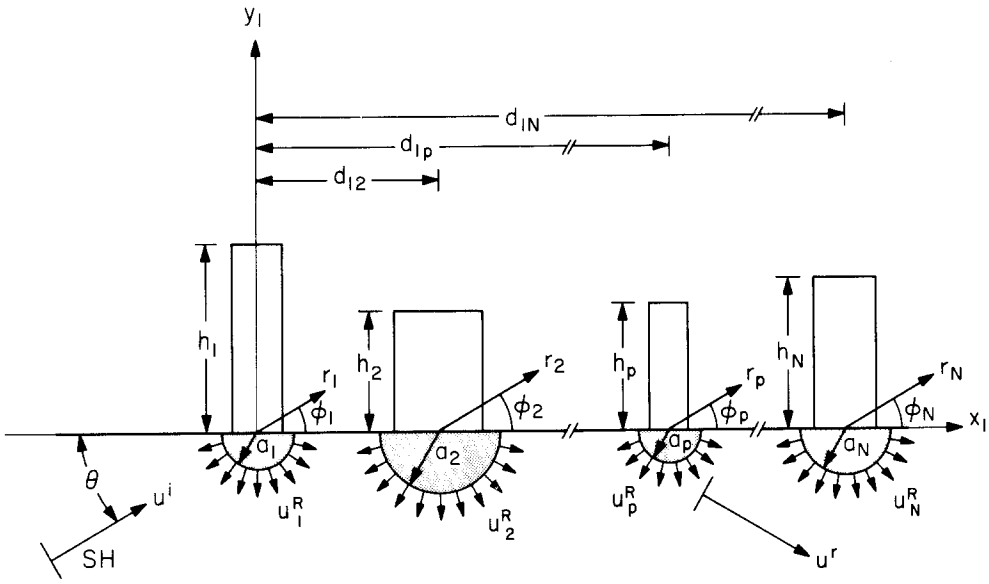

FIG. 1. The arrangement of structures and the coordinate systems.

chosen the coordinates for the first foundation (x_1, y_1) or (r_1, ϕ_1) as the reference, the coordinates of the other foundations located at distances d_{1p} may be expressed in terms of (x_1, y_1) by the transformation formulas

$$\begin{aligned} x_p &= x_1 - d_{1p} \\ y_p &= y_1 \end{aligned} \quad \text{where} \quad \begin{aligned} x_p &= r_p \cos \phi_p \\ y_p &= r_p \sin \phi_p \end{aligned}, \quad \text{and} \quad d_{11} = 0. \quad (1)$$

The model in Figure 1 clearly represents an extension of the models studied by Luco (1969) and Trifunac (1972).

Incident Ground Motion

We assume that the excitation consists of harmonic plane SH waves with an amplitude of 1 and the angle of incidence, θ, which is measured counterclockwise from the x-axis to

the normal of the plane wave front (Figure 1). The resulting free-field motion, u^{i+r}, in the half-space without the foundations then consists of the incident plane wave, u^i, plus the reflected plane wave, u^r, from the free surface. The free-field motion u^{i+r} given in the (x_1, y_1) coordinate system is then

$$u^{i+r}(x_1, y_1) = 2 \exp(i\omega t) \{\exp[-i(\omega/\beta)x_1 \cos\theta]\} \cos(\omega y_1/\beta \sin\theta) \tag{2}$$

where $\beta = \sqrt{\mu/\rho}$ is the shear-wave velocity in the soil. Using the transformation formulas (1), the expression (2) may be written in the (x_p, y_p) coordinate system as

$$u^{i+r}(x_p, y_p) = 2 \exp(i\omega t) \{\exp[-i(\omega d_{1p}/\beta) \cos\theta]\} \{\exp[-i(\omega/\beta) x_p \cos\theta]\} \times \cos(\omega y_p/\beta \sin\theta). \tag{3}$$

By omitting the time factor $\exp(i\omega t)$ for convenience in the remainder of this paper, the motion $u^{i+r}(x_p, y_p)$ may be represented by a series of circular cylindrical functions in the (r_p, θ_p) coordinates (Mow and Pao, 1971; Morse and Feshbach, 1953)

$$u^{i+r}(r_p, \phi_p) = 2 \exp[-i(\omega d_{1p}/\beta) \cos\theta] \left[\sum_{m=0}^{\infty} i^m \varepsilon_m J_m(Kr_p) \cos m\phi_p \cos m\theta\right] \tag{4}$$

where $\varepsilon_0 = 1$ and $\varepsilon_m = 2$ for $m \neq 0$.

Formulation of the Problem

The total displacement field, u, in the half-space and in the vicinity of the foundations is composed of the "free-field" motion u^{i+r} and the reflected waves u_i^R, $i = 1, 2, \ldots, N$ from each of the N foundations

$$u = u^{i+r} + \sum_{i=1}^{N} u_i^R. \tag{5}$$

The time-independent part of $u \exp(i\omega t)$ must satisfy the Helmholtz equation in each of the (r_p, ϕ_p) coordinate systems

$$\frac{\partial^2 u}{\partial r_p^2} + \frac{1}{r_p}\frac{\partial u}{\partial r_p} + \frac{1}{r_p^2}\frac{\partial^2 u}{\partial \phi_p^2} + K^2 u = 0 \tag{6}$$

where $K = \omega/\beta$ is the wave number. In addition to equation (6), boundary conditions must be satisfied in each of the (r_p, ϕ_p) coordinates. These conditions are: (a) the stress-free surface condition for the half-space

$$\sigma_{\theta z} = \frac{\mu}{r_p}\frac{\partial u}{\partial \phi_p} = 0 \qquad \text{at} \quad \begin{matrix}\phi_p = -\pi \\ \phi_p = 0\end{matrix} \quad \text{and} \quad r_p \notin R, \tag{7}$$

where R is the area occupied by the foundations, and (b) the continuous displacement condition at the interface between the foundations and the soil

$$u|_{r_p = a_p} = \Delta_p; \quad -\pi \leqq \phi_p \leqq 0, \tag{8}$$

where Δ_p is the displacement of the pth foundation. The Δ_p's depend on the soil-structure interaction of each of the N structures, the vibration of the other foundations, and the direction of the incoming waves θ.

The scattered waves from the jth foundation are assumed to be of the form

$$u_j^R = \sum_{n=0}^{\infty} A_n^j H_n^{(2)}(Kr_j) \cos n\phi_j, \qquad j = 1, 2, \ldots, N. \tag{9}$$

The boundary conditions (7) are then automatically satisfied by the total displacement field u, since the free-field motion u^{i+r} already satisfies the same condition. Also, by using only the Hankel function of the second kind $H_n^{(2)}(Kr_j)$, the scattered waves are of the divergent type.

In the boundary conditions (8) the N values of Δ_j are not yet known. However, by using the principle of superposition, the general form of the solutions for the scattered waves, u_j^R, from N foundations may be separated into $N+1$ parts to simplify the treatment of the boundary conditions. The determination of the unknown Δ_j's may then be postponed until the total interaction involving the N structures, N foundations, and the soil has been considered.

The scattered waves u_j^R can be separated as follows

$$u_j^R = W_j^{N+1} + \sum_{l=1}^{N} W_j^l \Delta_l, \tag{10}$$

where W_j^l, $l = 1, 2, \ldots, N+1$, all satisfy the Helmholtz equation (6). By substituting (10) into (5), we obtain

$$u(r_p, \phi_p) = u^{i+r}(r_p, \phi_p) + \sum_{j=1}^{N} \left\{ W_j^{N+1}(r_p, \phi_p) + \sum_{l=1}^{N} W_j^l(r_p, \phi_p)\Delta_l \right\}. \tag{11}$$

This expression will satisfy the boundary conditions (8), $u(r_p, \phi_p) = \Delta_p$ at $r_p = a_p$, if we set the boundary conditions for the $N+1$ problems into two categories

The $(N+1)$th problem

$$\sum_{j=1}^{N} W_j^{N+1}(r_p, \phi_p) + u^{i+r}(r_p, \phi_p) = 0 \qquad \text{at} \quad r_p = a_p. \tag{12}$$

The solution W_j^{N+1} for this case describes the scattered waves for the incident waves u^{i+r} with all of the N foundations held fixed.

First N problems

For $l = 1, 2, \ldots, N$

$$\sum_{j=1}^{N} W_j^l(r_p, \phi_p) = \delta_{lp} \qquad \text{at} \quad r_p = a_p. \tag{13}$$

The physical interpretation of the solutions of these N problems is that they describe the scattered wave fields when the lth foundation is moved with a displacement amplitude of 1 while the other foundations are held fixed.

The Solution of Wave-Scattering in the Soil

Having formulated the problem, we now consider the determination of the unknown coefficients A_n^j. We begin by noting that since u_j^R was divided into $(N+1)$ parts, A_n^j can also be divided and represented by

$$A_n^j = C_n^{j,N+1} + \sum_{l=1}^{N} C_n^{j,l} \Delta_l \tag{17}$$

where $C_n^{j,l}$, $l = 1, 2, \ldots, N+1$ are the coefficients of the solutions,

$$W_j^l = \sum_{n=0}^{N} C_n^{j,l} H_n^{(2)}(Kr_j) \cos n\phi_j. \tag{18}$$

To obtain the coefficients $C_n^{j,l}$, consider the following problems

The solution for W_j^{N+1}

From (17), the scattered wave from the jth foundation while it is held fixed is

$$W_j^{N+1}(r_j, \phi_j) = \sum_{n=0}^{N} C_n^{j,N+1} H_n^{(2)}(Kr_j) \cos m\phi_j.$$

But the boundary conditions (13) require that W_j^{N+1}, $j = 1, 2, \ldots, N$, be transformed into the (r_p, ϕ_p) coordinates. Therefore, the addition theorem may be used to transform the Bessel series from coordinates (r_j, ϕ_j), $j \neq p$, to (r_p, ϕ_p). Using the coordinate systems as defined in Figure 1, the transformation to the pth foundation from the right side, $j > p$ is

$$H_n^{(2)}(Kr_j) \cos n\phi_j = (-1)^n \left[\sum_{m=0}^{\infty} (\varepsilon_m/2) K_m^n(Kd_{pj}) J_m(Kr_p) \cos m\phi_p \right] \tag{19}$$

and from the left side, $j < p$ is

$$H_n^{(2)}(Kr_j) \cos n\phi_j = \left[\sum_{m=0}^{\infty} (-1)^m (\varepsilon_m/2) K_m^n(Kd_{pj}) J_m(Kr_p) \cos m\phi_p \right] \tag{20}$$

where

$$K_m^n(Kd_{pj}) = H_{n+m}^{(2)}(Kd_{pj}) + (-1)^m H_{n-m}^{(2)}(Kd_{pj}). \tag{21}$$

Equations (19), (20), and (21) are rearrangements of those given in Abramowitz and Stegun (1970). The transformations are not symmetrical because of the particular way in which the angles are defined in Figure 1.

With equations (19) to (21), the boundary conditions (13) for the $(N+1)$th problem may now be applied at (r_p, ϕ_p). The expressions for $p = 1, 2, \ldots, N$, which involve the unknowns $C_m^{p,N+1}$, are

$$\begin{aligned} 0 = {} & \left[2 \sum_{m=0}^{\infty} i^m \varepsilon_m J_m(Ka_p) \cos m\theta \right] \exp\left[-i(\omega/\beta) d_{1p} \cos\theta \right] + \sum_{m=0}^{\infty} C_m^{p,N+1} H_m^{(2)}(Ka_p) \cos m\phi_p \\ & + (1-\delta_{p1}) \sum_{j=1}^{p-1} \left[\sum_{n=0}^{\infty} C_n^{j,N+1} \sum_{m=0}^{\infty} (-1)^m (\varepsilon_m/2) K_m^n(Kd_{pj}) J_m(Ka_p) \cos m\phi_p \right] \\ & + (1-\delta_{pN}) \sum_{j=p+1}^{N} \left[\sum_{n=0}^{\infty} C_n^{j,N+1} (-1)^n \left[\sum_{m=0}^{\infty} (\varepsilon_m/2) K_m^n(Kd_{pj}) J_m(Ka_p) \cos m\phi_p \right] \right]. \end{aligned} \tag{22}$$

Using the orthogonal properties of the cosine functions, equation (22) may be separated to yield an infinite number of simultaneous equations as follows:

For the harmonic $\cos m\phi_p$, $j = 1, 2, \ldots, N$; $m = 0, 1, 2, \ldots$

$$\begin{aligned} & (1-\delta_{p1}) \sum_{j=1}^{p-1} \left[\sum_{n=0}^{\infty} (-1)^m C_n^{j,N+1} K_m^n(Kd_{pj}) \right] + C_m^{p,N+1} \left(\frac{2}{\varepsilon_m} \right) \left(\frac{H_m^{(2)}(Ka_p)}{J_m(Ka_p)} \right) \\ & + (1-\delta_{pN}) \sum_{j=p+1}^{N} \left[\sum_{n=0}^{\infty} (-1)^n C_n^{j,N+1} K_m^n(Kd_{pj}) \right] = -4i^m \cos m\theta e^{-i(\omega/\beta) d_{1p} \cos\theta}. \end{aligned}$$

$$p = 1, 2, \ldots, N; \; m = 0, 1, 2, \ldots \tag{23}$$

The first term on the left side of equation (23) represents the contribution of scattered waves from the foundations 1 through $p-1$, i.e., the foundations to the left of the pth foundation, while the third term represents the contributions from foundations $p+1$ through N, on the right side. As one would expect, these contributions to the interaction would be small if the parameter d_{pj} is large compared to $a_{\max}$. In such cases, the second

term dominates the left side of (23) because $|H_m^{(2)}(Ka_p)| \gg |K_m^n(Kd_{pj})J_m(Ka_p)|$ for $d_{pj} \gg a_p$. Therefore, neglecting the small term contributions, the problem reduces to the solution for a single foundation model.

After some manipulations, an infinite matrix results from equation (23)

$$A\mathbf{x}^{N+1} = \mathbf{b}^{N+1} \tag{24}$$

where

$$\mathbf{x}^{N+1} = \{C_0^{1,N+1} \ldots C_0^{p,N+1} \ldots C_0^{N,N+1} | C_1^{1,N+1} \ldots C_1^{p,N+1} \ldots C_1^{N,N+1} | \ldots | C_n^{1,N+1} \ldots C_m^{p,N+1} \ldots C_m^{N,N+1} | \ldots \}^T$$

or as written in indicial form

$$x^{N+1}_{(Nxq+p)} = \{C_q^{p,N+1}\} \tag{25}$$

$$b^{N+1}_{(Nxs+r)} = -\{4i^s \exp[-i(\omega/\beta)\, d_{1r} \cos\theta] \cos s\theta\} \tag{26}$$

$$A_{(Nxs+r),(Nxq+p)} = \frac{2}{\varepsilon_q} \frac{H_q^{(2)}(Ka_p)}{J_q(Ka_p)} \delta_{sq}\delta_{pr} + (1-\delta_{pr}) \begin{cases} (-1)^s K_s^q(Kd_{pr}), & \text{if } p < r \\ (-1)^q K_s^q(Kd_{rp}), & \text{if } p > r \end{cases} \tag{27}$$

Numerically, the infinite matrix equation (24) cannot be solved. Therefore, it is necessary to reduce it, if possible, to one of finite dimensions by taking advantage of certain properties of its coefficients.

For low frequencies, i.e., long incident waves, only lower order harmonics in the series (17) are required to describe the displacement field. Therefore, the coefficients, $C_n^{j,N+1}$, decrease rapidly, and the coefficients for large n do not affect those for small n appreciably. Hence, the infinite matrix may be reduced to one with finite dimensions. However, more terms in the infinite series are required when the frequency of excitation is large or when the size of the foundations differ greatly from each other. In the former case, high harmonics are required to describe the rapid changes of surface displacements caused by the short waves; while in the latter case, high harmonics are required to describe the sharp variation on the interface of the large foundations because of the short waves radiated by their smaller neighbors.

As an example, the number of terms used to calculate the coefficients for a two-body system with equal size foundations is approximately

$$\text{NUMBER OF TERMS} \simeq 5+2(Ka).$$

Four-place accuracy of the series solution has been achieved by comparing it with the series that had one additional term.

The solutions for W_j^l, $l = 1, 2, \ldots, N$

For these cases, the solutions are written in the form

$$W_j^l = \sum_{n=0}^{N} C_n^{j,l} H_n^{(2)}(Kr_j) \cos m\phi_j. \tag{28}$$

The "boundary condition" for (28) is given by the expression (12) and it is nearly the same as (13) except that $-u^{i+r}$ is replaced by δ_{lp}. Hence, the harmonic separation of this boundary condition gives

$$(1-\delta_{p1}) \sum_{j=1}^{p-1} \left[\sum_{n=0}^{\infty} (-1)^m C_n^{j,l} K_m^n(Kd_{pj}) \right] + C_m^{p,l} \left(\frac{2}{\varepsilon_m} \right) \left(\frac{H_m^{(2)}(Ka_p)}{J_m(Ka_p)} \right) + (1-\delta_{pN}) \sum_{j=p+1}^{N} \left[\sum_{n=0}^{\infty} (-1)^n C_n^{j,N+1} K_m^n(Kd_{pj}) \right] = \frac{2\delta_{m0}}{J_0(Ka_l)} \tag{29}$$

Since (29) is of the same form as (23), the matrix A in the expression $A\mathbf{x}^l = \mathbf{b}^l$ remains the same. Here, the first and third terms of (29) are the contributions from the neighboring fixed foundations, while the pth is being displaced with a unit amplitude. Again, for the case where $d_{pj} \gg a_p$, the matrix A becomes nearly diagonal, and the solution of the problem becomes that of a single foundation.

To complete the rearrangement of (29) in matrix form, define the vectors $\mathbf{x}^l$ and $\mathbf{b}^l$ as

$$x^l_{(Nxq+p)} = \{C_q^{p,l}\} \tag{30}$$

$$b^l_{(Nxs+r)} = 2\delta_{lr}/J_0(Ka_r). \tag{31}$$

Since the matrix A is the same as that of equation (27), the same criterion, discussed above, can be used to choose the size of the "finite" matrix.

Motion of the Foundations

The foundation displacements Δ_j can now be determined by balancing the forces exerted on the jth foundation: (1) f_i^s, the force generated by the soil and caused by the incident waves and the motion of the neighboring foundations; (2) f_i^W, the shear force created by the base of the structure; (3) the inertia force of the rigid foundation with mass $(M_0)_j$ whose acceleration is $-\omega^2\Delta_j \exp(i\omega t)$.

The force balance for the pth foundation then becomes

$$-\omega^2\Delta_p(M_0)_p = -(f_p^s + f_p^W) \qquad p = 1, 2, \ldots, N. \tag{32}$$

With the expression for the stresses at the pth foundation as

$$\sigma_{rz} = \mu\frac{\partial u}{\partial r_p} = \mu\frac{\partial}{\partial r_p}\left[u^{i+r}(r_p, \phi_p) + \sum_{j=1}^{N}\left\{W_j^{N+1} + \sum_{l=1}^{N} W_j^l\Delta_l\right\}\right], \tag{33}$$

the soil force f_p^s is expressed as

$$f_p^s = -\int_{-\pi}^{0} \sigma_{rz}|_{r_p=a_p}\, a_p d\phi_p. \tag{34}$$

Integration from $-\pi$ to 0 eliminates all harmonics except the zeroth. It is convenient to define f_p^s as

$$f_p^s = \mu\pi S_p + \mu\pi\sum_{l=1}^{N} K_{pl}\Delta_l \tag{35}$$

where $\mu\pi S_p$ is the force exerted by the soil on the pth foundation, while all foundations are held fixed. S_p may be expressed in terms of the coefficients $C_n^{j,N+1}$ as follows

$$\begin{aligned} S_p = Ka_pJ_1(Ka_p)\Bigg\{&2\exp[-i(\omega/\beta)]d_{1p}\cos\theta \\ &+ C_0^{p,N+1}\frac{H_1^{(2)}(Ka_p)}{J_1(Ka_p)} + (1-\delta_{p1})\sum_{j=1}^{p-1}\sum_{n=0}^{\infty} C_n^{j,N+1}H_n^{(2)}(Kd_{pj}) \\ &+ (1-\delta_{pN})\sum_{j=p+1}^{N}\sum_{n=0}^{\infty}(-1)^n C_n^{j,N+1}H_n^{(2)}(Kd_{pj})\Bigg\}. \end{aligned} \tag{36a}$$

The matrix K_{pl} represents the force exerted on the pth foundation, while only the lth

foundation is moved with a unit displacement,

$$K_{pl} = Ka_p J_1(Ka_p)\left\{C_0{}^{p,l}\frac{H_1{}^{(2)}(Ka_p)}{J_1(Ka_p)} + (1-\delta_{p1})\sum_{j=1}^{p-1}\sum_{n=0}^{\infty} C_n{}^{j,l}H_n{}^{(2)}(Ka_p)\right.$$
$$\left. + (1-\delta_{pN})\sum_{j=p+1}^{N}\sum_{n=0}^{\infty}(-1)^n C_n{}^{j,l}H_n{}^{(2)}(Ka_p)\right\}. \tag{36b}$$

To compute the force $f_p{}^W$, elastic shear walls with no damping are assumed to be the structures of interest in this problem. The shear walls satisfy the one-dimensional wave equation, and the base shear force of the walls subjected to a base-displacement of $\Delta_p \exp(i\omega t)$ is then (Luco, 1969)

$$f_p{}^W = -\omega^2(M_b)_p\left[\frac{\tan(K_b h)_p}{(K_b h)_p}\right]\Delta_p \tag{37}$$

where $(K_b)_p$ is the building's wave number, h_p is the height, and $(M_b)_p$ is the mass of the pth wall.

Substituting (35), (36), and (37) into (32), the force balance of all contributing forces is then

$$\omega^2\Delta_p(M_0)_p = -\omega^2(M_b)_p\left[\frac{\tan(K_b h)_p}{(K_b h)_p}\right]\Delta_p + \mu\pi\left\{S_p + \sum_{l=1}^{N} K_{pl}\Delta_l\right\}$$
$$p = 1, 2, \ldots, N. \tag{38}$$

Dividing (38) by $\mu\pi Ka_p$ and introducing the parameter $(M_s)_p = \frac{1}{2}\rho\pi a_p{}^2$, which is the mass per unit length of the soil replaced by the pth foundation, (38) becomes

$$\frac{(Ka_p)^2}{2}\left[\left(\frac{M_0}{M_s}\right)_p + \left(\frac{M_b}{M_s}\right)_p\frac{\tan(K_b h)_p}{(K_b h)_p}\right]\Delta_p - \sum_{l=1}^{N} K_{pl}\Delta_l = S_p$$
$$p = 1, 2, \ldots, N. \tag{39}$$

Equations (39) constitute N equations for the N unknowns, Δ_p. Hence, the foundation displacements Δ_p are uniquely determined by solving this set of simultaneous equations.

The Nature of the Interactions

The interactions of two or more structures are now considered by studying the numerical results presented in the figures which follow. The results shown in these figures depend mainly on the angle of the incident wave, θ, and four other dimensionless parameters:

1. $\omega a_p/\beta = Ka_p \equiv \eta_p$, the dimensionless frequency which compares the wavelength of the incident wave to the size of the pth foundation. To describe a system of foundations with different sizes, the maximum radius will be chosen as the reference, and the parameter $\omega a_{\max}/\beta$ will be used in plotting the figures. (The abbreviation of WA/B is used in place of $\omega a_{\max}/\beta$ in the figures.)
2. $(M_0)_p/(M_S)_p$, the ratio of the mass of the foundation to the mass of the soil replaced by the foundation. For all the cases studied in this paper, this ratio has been equated to 1.
3. $(M_b)_p/(M_S)_p$, the ratio of the mass of the pth shear wall to the mass of the soil replaced by the pth foundation.
4. $\varepsilon_p = (K_b h)_p/Ka_p$. This ratio describes the flexibility and the relative height of a shear wall. Larger values of ε indicate taller and/or more flexible walls, while $\varepsilon = 0$ implies a rigid structure or one with all its weight ($h_p = 0$) located at the base.

One of the interesting results that can be derived from the solution of equations (39) is represented by the displacements Δ_p of the foundations. In the figures that follow, amplitudes $|\Delta_p|$ have been plotted versus the dimensionless frequency WA/B ($A \equiv a_{\max}$) and are identified by a dashed line or a solid line. All of these amplitudes approach the low-frequency limit of $|\Delta_p| = 2$ (the displacement amplitude of the surface of half-space due to an incident SH-wave with amplitude 1) as $WA/B \to 0$.

Another characteristic of the foundation displacement Δ_p is that it becomes zero when the flexible pth shear wall is being excited at its fixed-base natural frequencies, $(K_b h)_p = (2n+1)\pi/2$, $n = 0, 1, 2, \ldots$, or by using relation (40), Δ_p is zero at

$$\frac{\omega a_{\max}}{\beta} = \frac{(2n+1)\pi}{2\varepsilon_p}\left(\frac{a_{\max}}{a_p}\right). \tag{41}$$

Δ_p has no finite zeroes if $\varepsilon_p = 0$. The occurrence of the zeroes of Δ_p has been explained by Luco (1969) and Trifunac (1972). It is that during the steady excitation of incident plane SH waves at the resonant frequencies of equation (41), the foundations behave as a node in a standing wave pattern.

The envelope of the response for a single wall placed on a half-space, $|\Delta_e|_p$, is plotted on the same graph as the foundation displacements $|\Delta_p|$. This envelope, $|\Delta_e|_p$, provides an upper limit for the response of the pth foundation if it is the only structure on the half-space, so it may be used to indicate the strength of the additional interaction effects caused by the presence of other structures. These envelopes resemble a hyperbola and are described by the equation (Trifunac, 1972)

$$|\Delta_e|_p = \left[J_1(Ka_p) - \frac{J_0(Ka_p)H_1^{(2)}(Ka_p)}{H_0^{(2)}(Ka_p)}\right]\left[\frac{J_0^2(Ka_p)+Y_0^2(Ka_p)}{Y_0(Ka_p)J_1(Ka_p)-Y_1(Ka_p)J_0(Ka_p)}\right]. \tag{42}$$

These envelopes have been plotted with the same type of lines as $|\Delta_p|$ in the subsequent figures.

Interaction of Two Walls

Displacements, Δ_p, during the steady interaction between the two walls are illustrated in Figures 2, 3, and 4; they are designated by "DELTA". Each of these figures consists of parts (a), (b), and (c) which present the effects of different separation distances; each part also includes 5 graphs which correspond to the angles of incidence $\theta = 0°$, 45°, 90°, 135°, and 180°. (Note: θ is written as THETA in these graphs.) These figures have been arranged so that the influence of the angle of incidence and the separation distance can be studied together.

For the two cases shown in Figures 2 and 3, the values of ε_p are taken to be zero so that the interaction effects of only the foundations can be more clearly shown. In this way the complications introduced by the tall vibrating walls are eliminated.

An interesting interaction phenomenon occurs when the incident wave travels with a shallow angle of incidence. The wall in front acts as a shield for the wall behind, but the latter may amplify the excitation for the former. This shielding effect is most evident in Figure 3 where the size of wall 1 is 5 times that of wall 2. (The numbering system used here is the same as that used in Figure 1.)

For incident wave angles, THETA = 0° or 45°, and small wall separation distances, the smaller wall 2 moves with nearly the same displacement as the larger wall 1. The additional amplification effects caused by the smaller wall are negligible in this case because of the massiveness of the larger wall. The situation is reversed, however, when the waves are coming at an angle THETA = 135° or 180°. Now the "front wall" is much smaller than

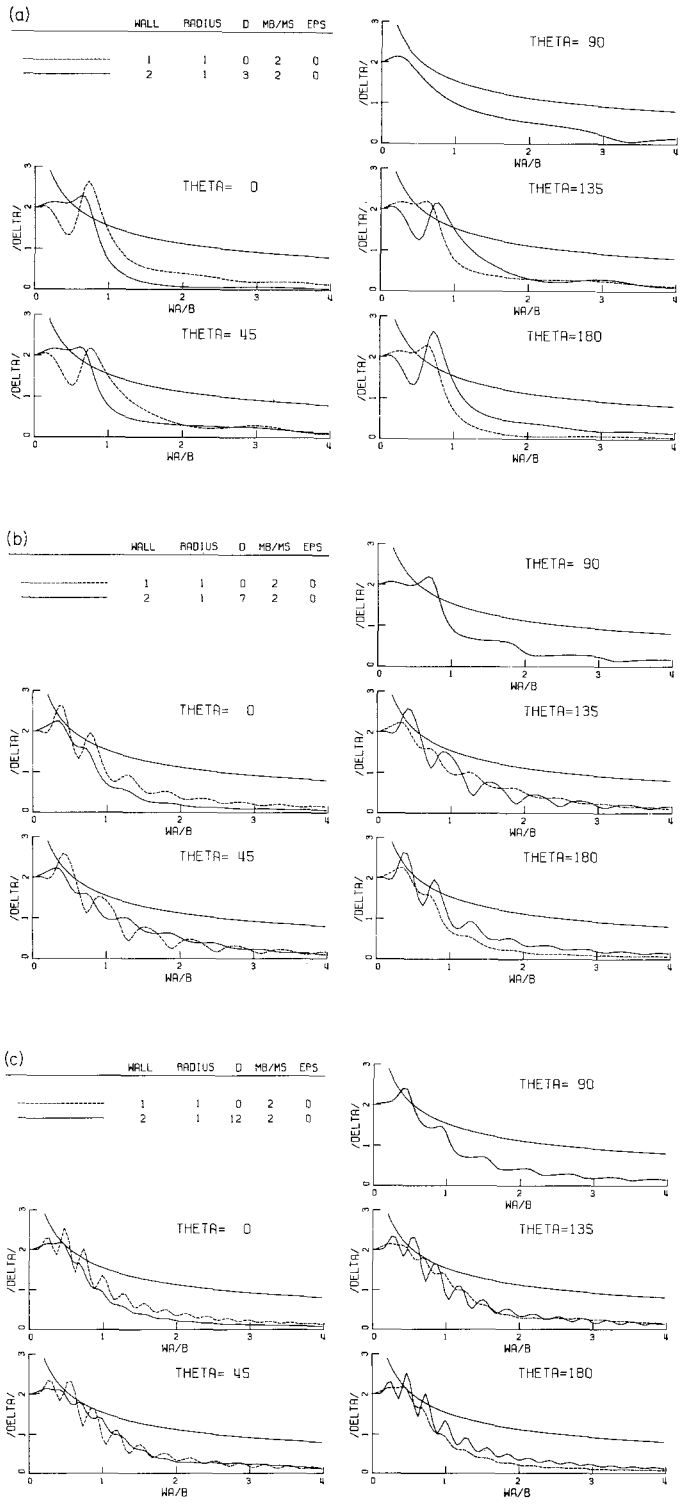

FIG. 2. The foundation displacement of two identical structures.

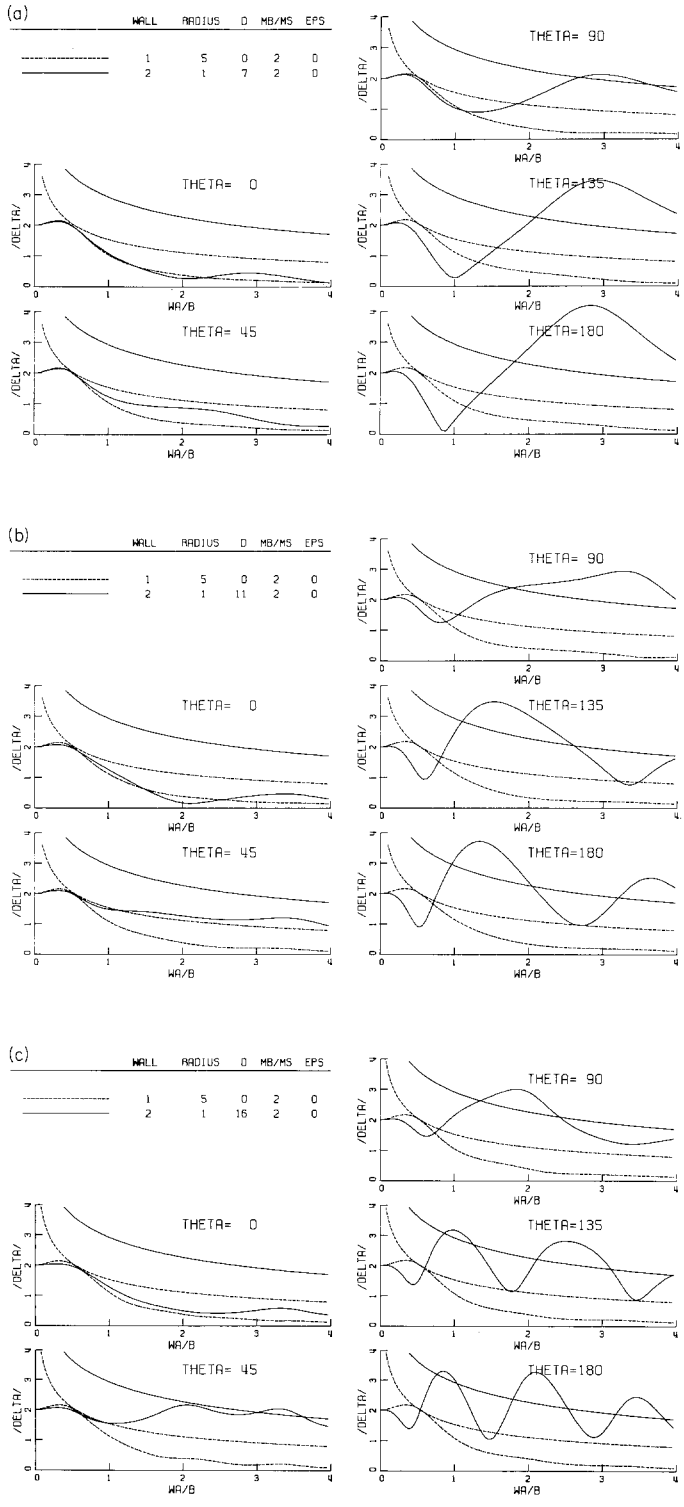

FIG. 3. The foundation displacements of two structures with foundation-size ratio of 5 to 1.

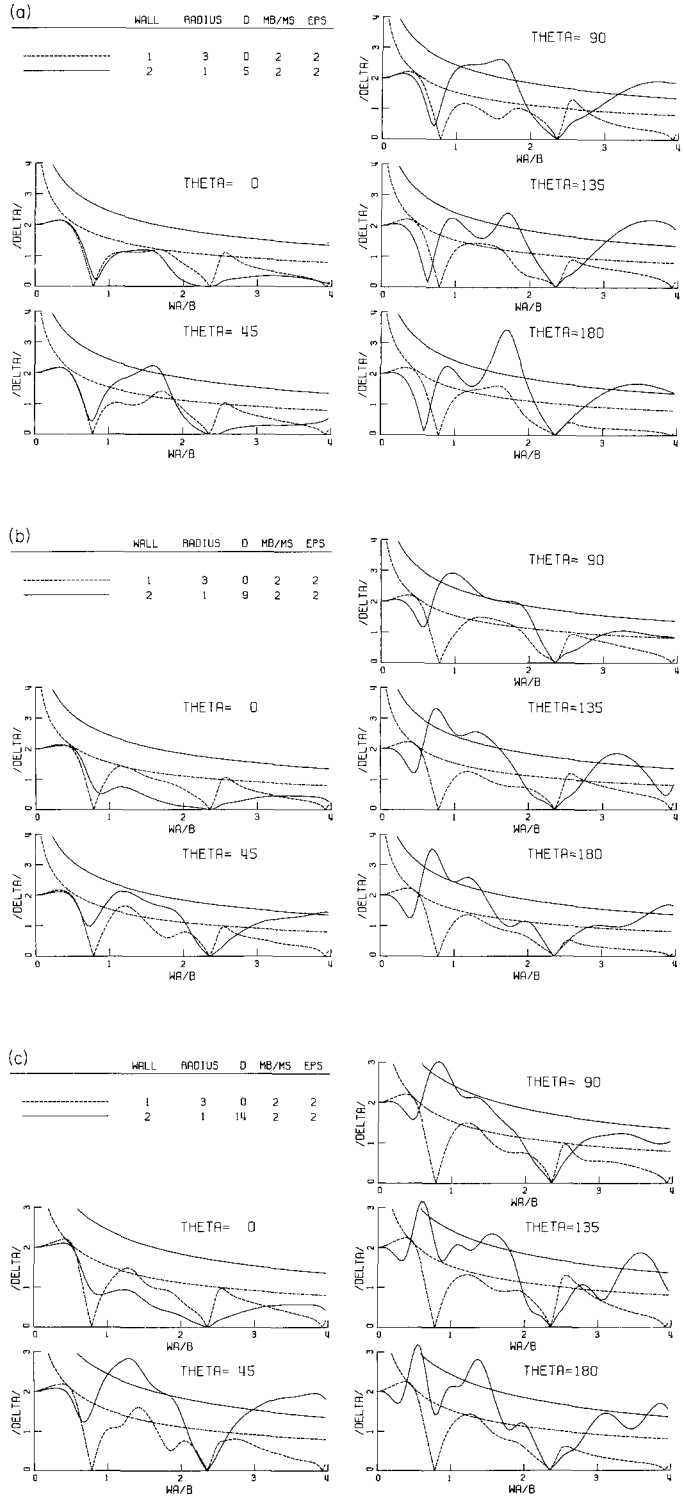

FIG. 4. The foundation displacements of two structures with foundation-size ratio of 3 to

the "back wall"; here, the "front wall" means the first wall to be hit by the incident waves. In this case, the shielding effect provided by the "front wall" is negligible, while the amplifying effect caused by the "back wall" is overwhelming.

For the cases where the "front wall" is of comparable size or much smaller than the "back wall", the response of the front foundation dips down to a small value of Δ before it rises to a level exceeding the envelope curve of equation (42) at some higher frequency. This dip in foundation response amplitude for the front wall is greater when this foundation is smaller than the back foundation. The response is nearly zero at this point for the case described in Figure 3.

This phenomenon can be explained by the standing waves generated by the interference of the incident and the reflected wave from the larger back wall. For certain frequencies and/or distances, the smaller wall may be situated on a node and experience pure torsional excitation. This behavior can also be explained qualitatively by a vibration absorber example. Consider the following simplified model of the two-foundation system. The spring constants k_1, k_2, and k_{12} depend upon the soil properties and, hence, are

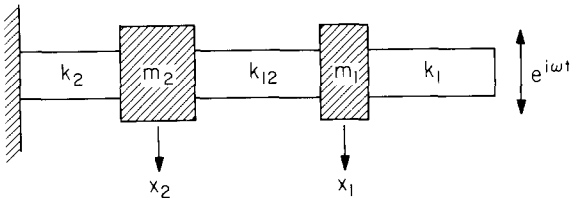

FIG. 5. A simplified model of the two-structure system.

highly frequency-dependent because of the geometrical configuration of the foundations. The displacements resulting from simple harmonic excitation are

$$\begin{cases} x_1 = \dfrac{k_1(k_2+k_{12}-\omega^2 m_2)}{\Delta} \exp(i\omega t) \\ x_2 = \dfrac{k_1 k_{12}}{\Delta} \exp(i\omega t) \end{cases}$$

where

$$\Delta = (k_1+k_{12}-\omega^2 m_1)(k_2+k_{12}-\omega^2 m_2)-k_{12}^2. \tag{43}$$

Note that if $k_2+k_{12} = \omega_*{}^2 m_1$ or $\omega_* = (k_2+k_{12})^{1/2}/m_2$, the response of m_1, x_1 becomes zero and $x_2 = -k_1/k_{12} \exp(i\omega t)$. Hence, m_1 is stationary at $\omega = \omega_*$, while m_2 is moving in an opposite direction from the excitation; so the forces on either side of m_1 eliminate each other, and m_1 is located on a node of a "standing wave" pattern. The system in Figure 5 is, of course, far too simplified to describe the phenomenon of the interactions in detail because the scattering from the foundations introduces "damping" into the system and the wave propagation is two-dimensional. However, the intuitive physical explanation of this interaction problem is well represented by this model.

The spring constant k_{12} can be visualized as the soil joining the two foundations, so that as the separation becomes large, the interaction is weaker, and $k_{12} \to 0$ as $d_{12} \to \infty$. The frequency ω_* becomes smaller and the dip occurs at lower frequencies for larger separations.

The troughs and the crests in the response of Δ_p for the front foundation may be better visualized by studying Figures 6, 7, and 8, where the amplitudes of surface displacements in the vicinity of the two foundations are plotted against the dimensionless frequency, η,

	WALL	RADIUS	D	M_b/M_s	EPS
$\theta = 135°$	1	2	0	2	0
	2	1	5	2	0

	WALL	RADIUS	D	M_b/M_s	EPS
$\theta = 180°$	1	2	0	2	0
	2	1	5	2	0

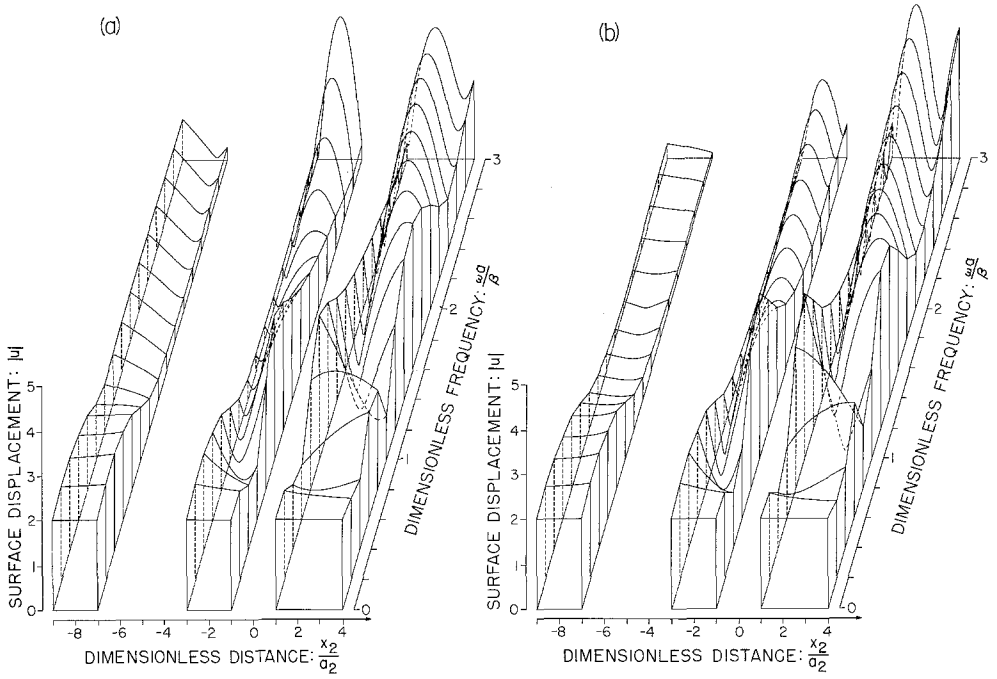

FIG. 6. The ground-surface displacement around two structures. Foundation-size ratio is 2 to 1, separation distance is 5.

	WALL	RADIUS	D	M_b/M_s	EPS
$\theta = 90°$	1	2	0	2	2
	2	1	4	2	3

	WALL	RADIUS	D	M_b/M_s	EPS
$\theta = 180°$	1	2	0	2	2
	2	1	4	2	3

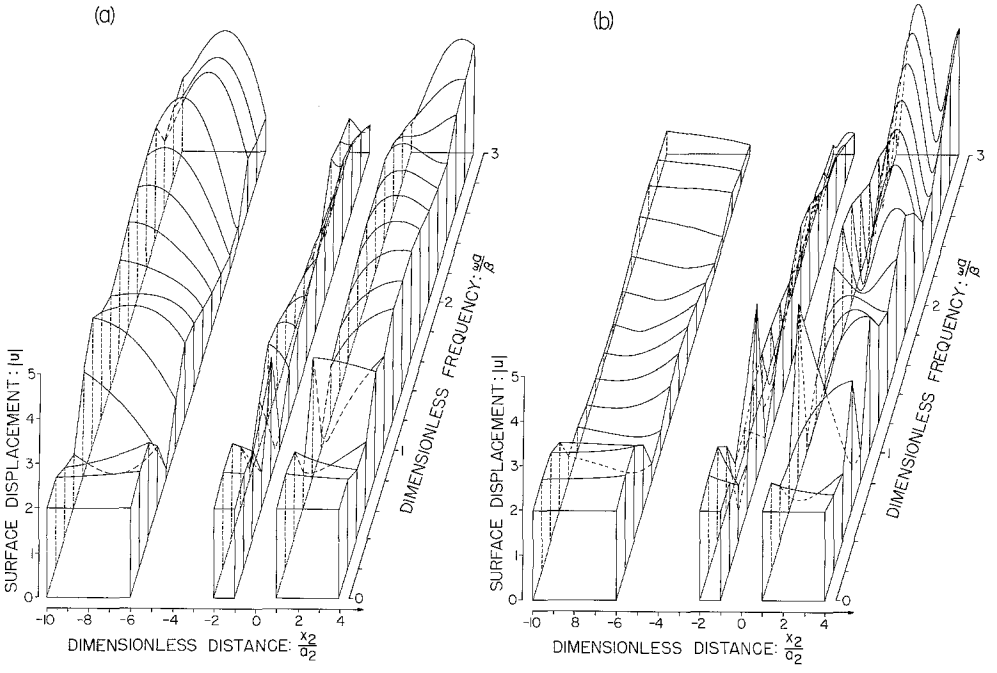

FIG. 7. The ground-surface displacement around two structures. Foundation-size ratio is 2 to 1, separation distance is 4.

and the dimensionless distance x/a. The definition of dimensionless parameters used in these figures are identical to those discussed previously.

The foundation size ratio for all cases presented in Figures 6, 7, and 8 is 2 to 1. Figure 6 illustrates the scattered wave patterns around the two foundations for THETA = 135° and 180°, both of which have rigid walls, i.e., for $\varepsilon = 0$. Figure 7 illustrates the effect of vertically incident waves in part (a), and the effect of horizontally incident waves in part (b); both shear walls considered here are flexible and tall. The surface displacement plots of Figure 8 show the weaker interaction with a larger separation distance.

In Figure 6b, the phenomenon described by a simple model in Figure 5 can be observed. The first trough of the response Δ_2 of the smaller foundation occurs at $\omega A/\beta \cong 0.4$. At

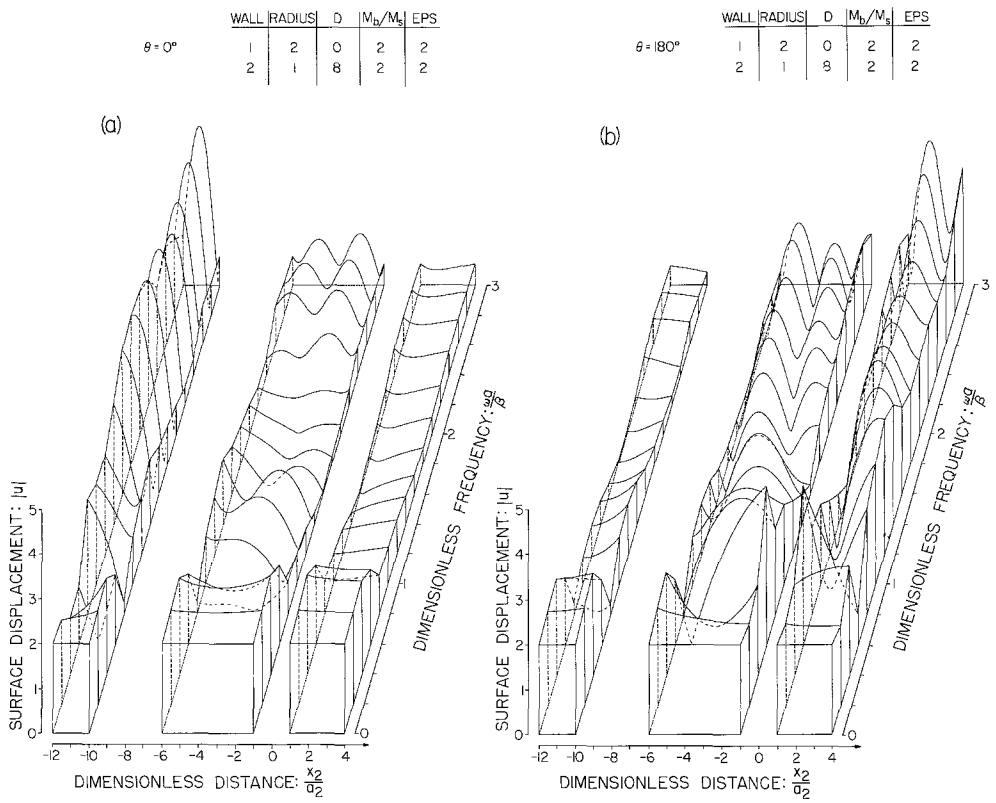

FIG. 8. The ground-surface displacement around two structures. Foundation-size ratio is 2 to 1, separation distance is 8.

that frequency, both foundations are moving in phase with foundation 1 and have large amplitudes. Not far to the right of foundation 2, there is a point with small displacement. This is where the displacements on either side change direction and, hence, the point pivots the movement of both walls. If the foundation size ratio is much greater than 2 to 1, e.g., 5 to 1, the presence of the smaller foundation can almost be ignored when studying the response of large foundations. Also, for a certain wavelength of incident waves, the motion of the smaller foundation may be located on a node of a standing wave pattern and remain stationary.

The crest of the response Δ_2, which follows the trough, occurs at $\omega A/\beta \cong 1.0$ in Figure 6b, and is created by the amplifying effect of wall 1. At this particular frequency, the two walls are nearly 180° out of phase, and the "node" is now located between the two

foundations. Because of the rapid change of phase in the vicinity of a "node", the ground motion at that point is essentially torsional. When the frequencies are higher than $\omega A/\beta \cong 1.5$, or when the wavelength of the incident wave becomes smaller than the separation distance, the interaction effects gradually disappear and the response of the foundations most likely does not exceed appreciably the envelopes for the response of a single foundation.

It is clear from the above discussion that the presence of two shear walls increases the complexity of response of each foundation and that the interference of waves scattered from the two foundations may lead to appreciable amplification of their base motions, Δ_p. It is beyond the scope of this paper to analyze in detail these amplifications caused by the building-soil-building interaction effects, but the general trends may nevertheless be

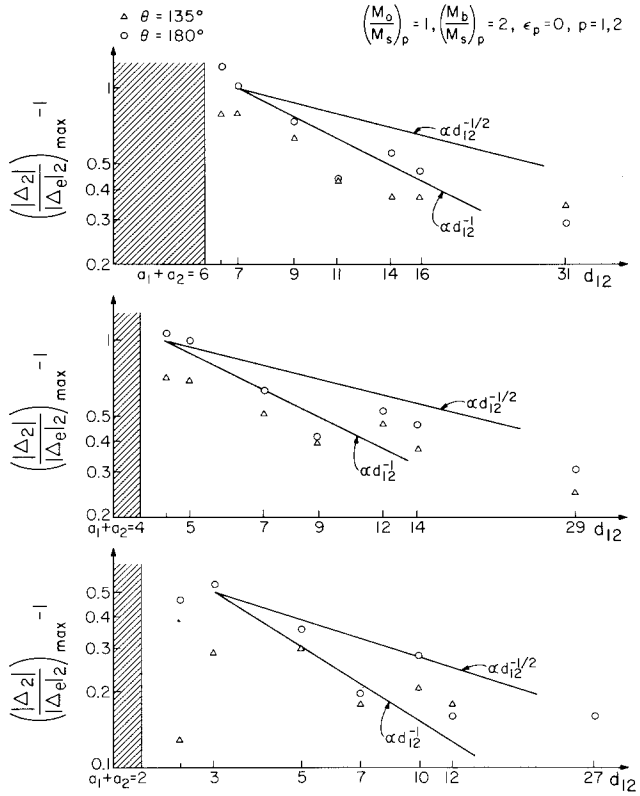

FIG. 9. The effect of separation distance on the amplifying effect of two-structure interaction.

extracted from several cases considered. These amplifications determined for three foundation-size ratios are presented in Figure 9 and are plotted versus the separation distance, d_{12}. Some of these results have been extracted from Figures 2 and 3.

The two sets of points in Figure 9 show the differences caused by the angle of incidence. Since wall 2 is smaller, the amplifying effects occur for $\theta > 90°$, e.g., $\theta = 135°$ and 180°. Because the waves scattered from the two foundations are of cylindrical type, one would expect that the peak amplitude $|\Delta_2|$ of small foundations would be related to its envelope $|\Delta_e|$ by $(|\Delta_2|/|\Delta_e|)_{\max} - 1 \approx \text{const.}/d_{12}^{1/2}$ when d_{12} is larger compared to $a_1 + a_2$. This is simply stating that $|\Delta_e|$ is entirely due to scattered, u^R, waves. Diffraction and interference effects for d_{12} small may alter this trend appreciably and in the limit for $d_{12} \to a_1 + a_2$, we have $(|\Delta_2|/|\Delta_e|)_{\max} - 1 \to 0$. It appears that the few points plotted in Figure 9

may be explained by these trends. It is clear, however, that the continuous representation of $(|\Delta_2|/|\Delta_e|)_{\max} - 1$ versus d_{12} should have numerous peaks and troughs which are caused by the interference of scattered field with the incident plane *SH*-waves. It is this interference that causes the apparent scatter of the few randomly selected points in Figure 9.

Interaction of Many Walls

The interaction which involves many foundations clearly becomes more complex as the number of foundations increases, but the solution presented in this paper should provide a simplified two-dimensional picture of what might occur in the densely constructed metropolitan areas where elongated buildings have been erected parallel to each other.

In Figures 10 and 11, foundation response $|\Delta_p|$ for three foundations with rigid walls have been presented. Figure 10 shows a case where one small wall is placed between two larger walls of 3 times its size, and $\varepsilon_p = 0$ for all three walls.

For the foundation response shown in Figure 10a, the two large outside walls behave the same way as though the smaller middle wall is absent. This conclusion results from comparison of $|\Delta_1|$ and $|\Delta_3|$ with $|\Delta_1|$ and $|\Delta_2|$ of Figure 2a where the response of two identical walls has been presented. However, at $WA/B \cong 1.8$, Δ_1 and Δ_3 are slightly altered and the response of the wall 2 is strongly excited for $d_{12} = 5$ and $d_{13} = 10$. In Figure 10b, the peak at $WA/B \cong 1.8$ has been translated to $WA/B \cong 0.85$, indicating that the "resonant frequency" of the small wall is highly dependent on the distance to the larger walls. For the case in Figure 9c, the separation distance is large so that the building-soil-building interaction effects cease to be prominent.

The interaction of three walls as described above can again be visualized by using a simplified model of springs and masses. Since the relative motions of the large outside walls are relatively small, the excitation can be considered to be such that m_1 and m_3 are moving with displacement $\exp(i\omega t)$ as shown in Figure 12. The "resonant frequency" of m_2 is therefore

$$(k_{12}+k_{23})^{1/2}/m_2. \tag{44}$$

When excited at that particular frequency, the motion of m_2 would become unbounded. But again, in the two-dimensional model, scattering of waves from the semi-cylindrical foundations reduces the response amplitude. As the separation distances d_{12} and d_{13} increase, the "spring constants" k_{12} and k_{23} decrease, and by equation (44), the "resonant frequency" also decreases. Therefore, the simplified model shown in Figure 12 quantitatively explains the translation of the peaks shown in Figure 10a and 10b when d_{12} and d_{13} become large.

Another case of interest is when a large wall is surrounded by smaller walls. Figure 11 presents such an example for three walls with the middle wall three times larger than the two outside walls. The distances d_{12} and d_{13} are the same as those used in Figure 10. Now the middle wall "drives" the outside walls because of its weight and size, and a totally different situation arises. As may be seen in Figure 11, the response of the large middle wall is not greatly affected by the smaller outside walls. But the smaller walls behave as if they were interacting with the large wall alone, i.e., one small wall contributes very little to the behavior of the other small wall. For horizontally incident waves, the response of the front wall is being amplified, while the back wall is being shielded. The large middle wall moves as if the other two are absent.

As indicated by the above analysis, the weight and size of the structure plays an important role in the interaction process. This suggests that the smaller structures in a

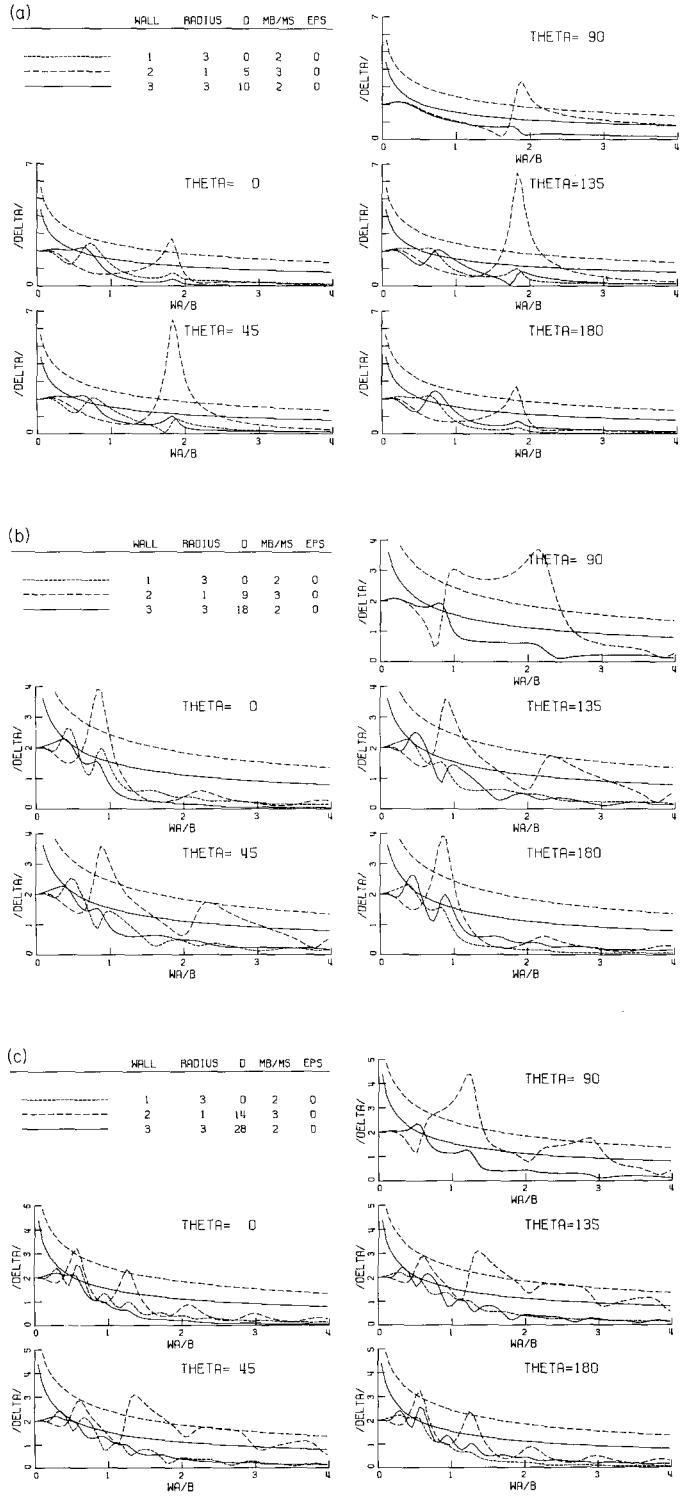

FIG. 10. The foundation displacements of three structures with foundation-size ratio of 3 to 1 to 3.

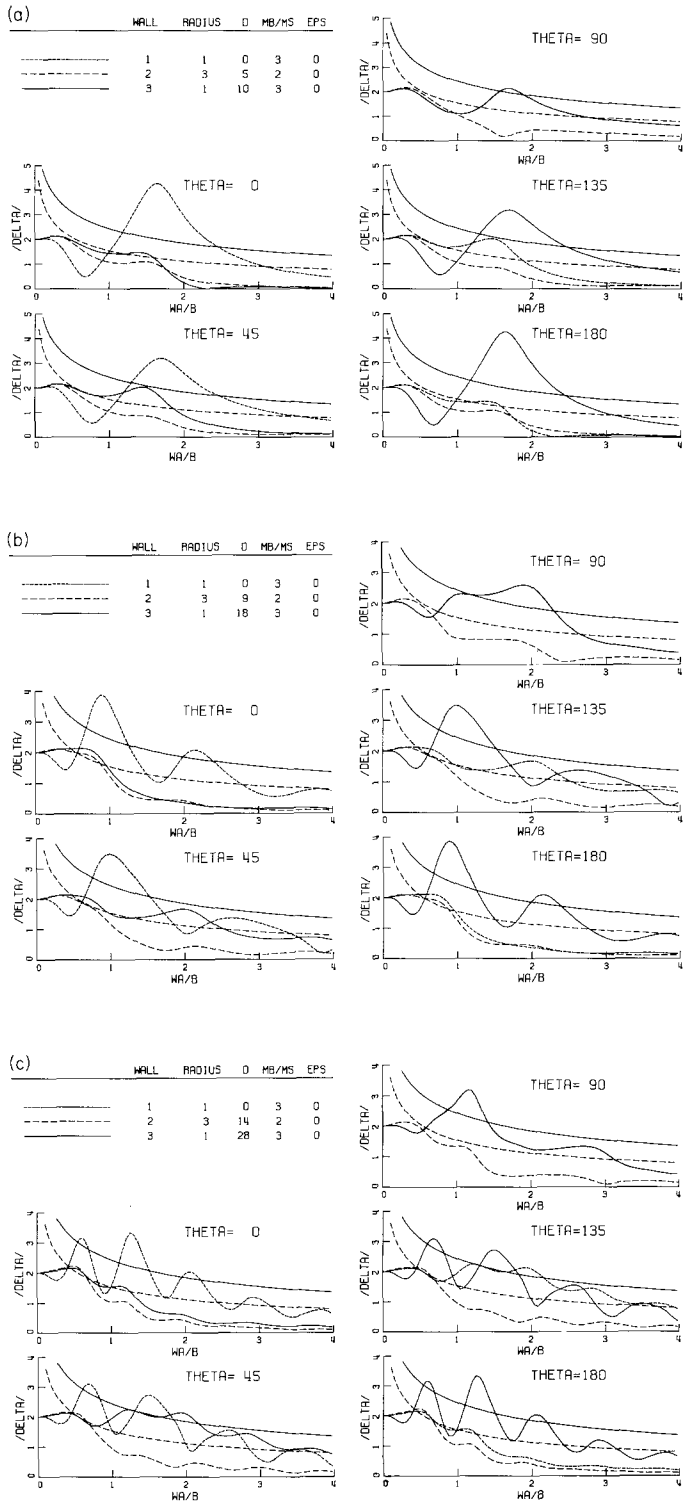

FIG. 11. The foundation displacements of three structures with foundation-size ratio of 1 to 3 to 1.

densely constructed area will probably receive the heavy "bombardment" of scattered waves from larger buildings.

Large amplitudes of response can also arise when many buildings of comparable size are closely grouped. Figure 13 presents an arrangement of five identical foundations, all of which support a rigid wall. In this particular case, we find that the amplitude $|\Delta_p|$ can exceed the single foundation envelope given by equation (42) by more than 200 per cent. We expect, however, that such building-to-building interaction effects will not be so prominent in three dimensions, because the geometrical radiative scattering of waves causes the "radiation damping" of the whole system to increase.

The Measurement of Earthquake Motions

In earthquake engineering, the measurement of the base motion of structures as well as the free-field motion is of interest. Considering the interaction effects discussed in the previous sections, the true measurement of the free-field motions might be difficult to realize. As shown by the surface displacement plots (of Figures 6, 7, and 8), the amplitude of surface motion is greatly altered from the free-field amplitude of 2. At some points, the displacements are near zero, while they are close to 4 at other locations. These rapid changes of displacement amplitudes are most evident for higher frequencies. The amplification of the surface displacement can be quite large even when caused by interaction at large distances, as shown, for example, in Figure 8.

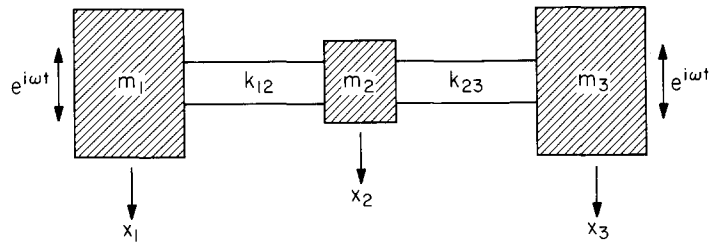

FIG. 12. A simplified model of the three-structure system.

An accelerogram recorded at the base of a structure may also be frequency filtered by the effects from neighboring large structures or structures of comparable size. As pointed out by Luco (1969), such records may be filtered around the natural frequencies of the structure. From the discussion of the interaction of many foundations, it now appears that it is possible to have "resonant frequencies" caused by the specific arrangement of the surrounding buildings. This suggests that the "resonant frequency" of a large structure may also be recorded in surrounding smaller structures as it dominates the behavior of the others. This effect can be observed in Figure 4, where the parameters are $a_1 = 3$, $a_2 = 1$, $\varepsilon_1 = 2$ and $\varepsilon_2 = 2$. By using equation (41), the response curve $|\Delta_1|$ should go to zero at $\omega a_{\max}/\beta = 3(2n+1)\pi/4$, $n = 0, 1, 2, \ldots$. In Figures 4a and 4b, the curve $|\Delta_2|$ also dips down to an amplitude of almost zero at the resonant frequency of the wall 1. When the large structure acts as a shield for the small structure, as in the case of $\theta = 0°$ and 45° in Figure 4, the small structure moves with nearly the identical displacements as that of the large structure. Of course, this behavior begins to change when the wavelength of the incident wave is less than that of the separation distance.

Conclusions

The antiplane response of a two-dimensional semi-cylindrical foundation is more com-

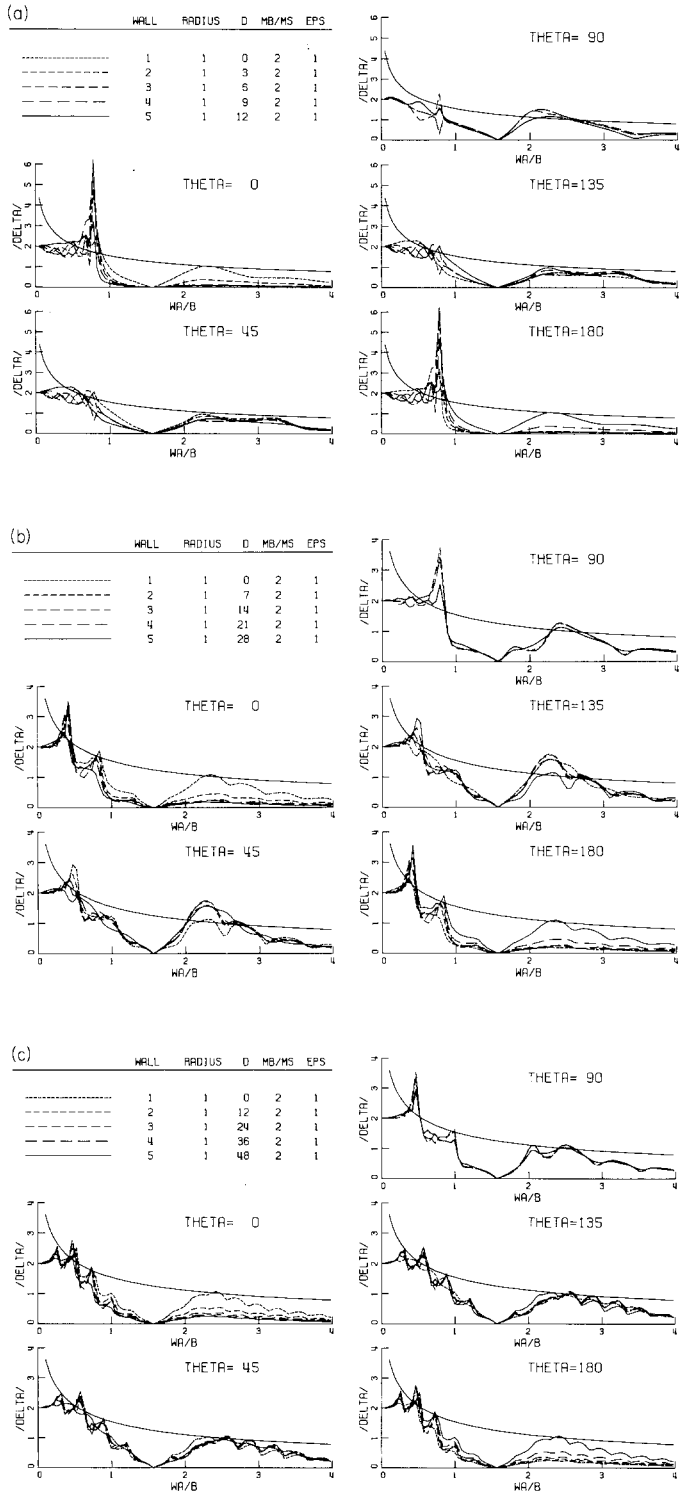

G. 13. The foundation displacements of five identical and equally spaced structures.

plicated and more unpredictable if many other foundations are present in the area. For selected frequencies the amplitude of the foundation response might differ from the theoretical prediction by 200 per cent or more if the multifoundation interaction effects are left out.

The structure-soil-structure interaction is especially prominent if the structure of interest is smaller and lighter than its neighbors; in which case, the following may occur:

1. If a small structure is located in front of one or more larger structures, while subjected to a horizontally incident plane *SH* wave, the motion of the foundation could be vastly changed from one frequency to another. These changes are mainly caused by the standing wave pattern created by the larger foundations behind. Also, if the smaller foundation is located at a node of a standing wave pattern, torsional type motion may occur.
2. If a small structure is located behind one or more larger structures, most of the incident wave energy may be scattered and the small structure will tend to move along with the same displacement as the larger one in front.
3. If a small structure is located between the two or many structures, resonating phenomena may occur if the waves scattered from the neighboring structures interfere constructively. The frequency of this resonance depends on the spacing and the arrangements of the entire system.

The interaction between buildings of comparable sizes may also cause the amplitude of response to become quite large for certain frequencies. These amplitudes also depend on the spatial arrangement of the buildings.

All of the above effects cause the foundation motion to be frequency filtered. Therefore, the motion observed at the base of a long structure could be quite different from the "free-field ground motion". The scattering of waves in the vicinity of the foundations can also alter the "free-field motion" appreciably.

Acknowledgments

We are indebted to P. C. Jennings and J. E. Luco for critical reading of the manuscript. We thank J. E. Luco for valuable comments and discussion which lead to significant improvements of this paper.

This research was supported by grants from the National Science Foundation and the Earthquake Research Affiliates Program at the California Institute of Technology.

References

Abramowitz, M. A. and I. A. Stegun (Editors) (1970). *Handbook of Mathematical Functions*, Dover, New York.

Liang, V. C. (1974). Dynamic response of structures in layered soils, *Ph.D. Thesis*, Massachusetts Institute of Technology, Cambridge, Mass.

Lee, T. H. and D. A. Wesley (1973). Soil-structure interaction of nuclear reactor structures considering through-soil coupling between adjacent structures, *Nucl. Eng. Design* **24**, 374–387.

Luco, J. E. (1969). Dynamic interaction of a shear wall with the soil, *J. Eng. Mech. Div., ASCE* **95**, EM2, 333–346.

Luco, J. E. and R. A. Westmann (1971). Dynamic response of circular footings, *J. Eng. Mech. Div., ASCE* **97**, 1381–1395.

Luco, J. E. and L. A. Contesse (1973). Dynamic structure-soil-structure interaction, *Bull. Seism. Soc. Am.* **63**, 1289–1303.

McCalden, P. B. (1969). Transmission of steady state vibrations between circular footings, *Ph.D. Thesis*, University of California at Los Angeles.

Mow, C. C. and Y. H. Pao (1971). The diffraction of elastic waves and dynamic stress concentrations, *RAND Report, R-482-PR.*

Morse, P. M. and H. Feshbach (1953). *Method of Theoretical Physics*, McGraw-Hill, New York.

Trifunac, M. D. (1972). Interaction of a shear wall with the soil for incident plane *SH*-waves, *Bull. Seism. Soc. Am.* **62,** 63–83.

Warburton, G. B., J. D. Richardson, and J. J. Webster (1971). Forced vibration of two masses on an elastic half space, *J. Appl. Mech., A.S.M.E.* **38,** 148–156.

Wong, H. L. and M. D. Trifunac (1974). Interaction of a shear wall with the soil for incident plane *SH*-waves: Elliptical rigid foundation, *Bull. Seism. Soc. Am.* **64,** 1825–1842.

EARTHQUAKE ENGINEERING RESEARCH LABORATORY
CALIFORNIA INSTITUTE OF TECHNOLOGY
PASADENA, CALIFORNIA 91125

Manuscript received November 11, 1974